

McLean Sec.11-11.3.2

Misato Fujii

11 Electronic imaging at infrared wavelength

- CCDs do not respond $>1.1\mu\text{m}$ due to the bandgap of silicon
 - ⇒ Different materials and techniques are required for the infrared range
- In this section, the development and impact of infrared array detectors are described

11.1 Introduction

- infrared observations are very important in astrophysics
 - the visible light from **distant objects** is redshifted to the infrared
 - able to see **the star-forming regions** surrounded in clouds of gas and dust
 - see **the center of the Milky Way** and reveal the nature of the central mass of the Galaxy
 - **cold interstellar material** emits far-infrared
 - low-energy infrared photons are emitted from **energy transitions in molecules** that involve quantized rotation and vibration states

11.1 Introduction

- optical-IR boundary
 - $<2.2\mu\text{m}$: background light comes mainly from OH emission in the atmosphere
 - $>2.2\mu\text{m}$: dominant source of background radiation is the thermal emission from the atmosphere and telescope components
 - wavelength range of infrared
 - Near-Infrared (NIR): $0.9\text{-}5.5\mu\text{m}$
 - Mid-infrared (MIR): $5\text{-}30\mu\text{m}$
 - Far-infrared (FIR): $3\text{-}200\mu\text{m}$
- observations at long wavelengths (MIR, FIR) are challenging from the ground but the interest from the stratosphere

11.1.1 Early history of infrared astronomy

- Sir William Herschel (1738-1822)
 - a thermometer placed just beyond the reddest end of a spectrum of sunlight
 - increased its temperature compared with other thermometers set off to the side
 - greater heating than any other location within the spectrum
 - "calorific rays": these unseen radiations, proved that they were refracted and reflected
 - "holes in the sky": irregularly shaped dark regions where MW stars seemed to vanish
 - recognized as dense clouds of gas and dust
- interstellar dust affects the blue light more than red light
 - **motivation for infrared studies**

11.1.2 The beginning of modern infrared astronomy

- major breakthroughs: after WW2
- **lead sulfide** (galena, **PbS**)
 - semiconductor with a fundamental bandgap of 0.41eV (room temperature)
 - drop to 0.826eV (4.3 μ m) at 4.2K
 - early 1960s: two-micron sky survey (TMSS, Neugebauer&Leighton)
 - detector: 8 separate PbS photoconductors in a pair-wise to remove background radiation
 - • “1st-magnitude” infrared sources (1965)
 - infrared objects at the center of MW, not seen in visible light (1968)
 - BN object (Orion Nebula) that is a very bright but optically invisible young star

11.1.2 The beginning of modern infrared astronomy

- liquid helium cooled **gallium-doped germanium (Ge:Ga) bolometer** (Frank Low, 1961)

- wavelength-independent response

- ⇒ longer wavelengths

- built detectors for 10 μ m and 21 μ m

- NASA Learjet (70 μ m), balloons and rockets



Learjet

<https://planetags.com/ja/blogs/planetags-blog/lear-jet-24-nasas-airborne-observatory>

→ • the discovery of an extended infrared-glowing cloud near the BN object in Orion at 22 μ m (Kleinmann-Low Nebula)(Kleinmann & Low 1967)

- some distant galaxies emitted far more infrared radiation than all other wavelengths combined (Kleinmann & Low 1970)

11.1.2 The beginning of modern infrared astronomy

- **indium antimonide (InSb)**: more sensitive photodiode
 - Mt. Lemon Infrared Observatory (1970s)
 - 1.5m infrared “flux collector” on Tenerife in the Canary Islands (1971)
 - study of southern hemisphere skies at Mt. Stromlo using a series of detectors (Hyland 1971)
 - infrared observations with a single element detector on the Anglo-Australian Telescope (Allen et al)
 - Kuiper Airborne Observatory (KAO) for better far-infrared observations
 - modified C-141A jet transport aircraft with a 91.5cm (36inch) Cassegrain telescope with operation at altitudes of up to 14km (45,000ft)
 - first detection of faint rings around Uranus
- new generation of **3-4m class telescopes** dedicated to infrared astronomy by 1979

11.1.3 The launch of IRAS

- Anglo-American-Dutch Infrared Astronomical Satellite
 - launch on 1983/1/25 and 10 months in operation
 - superfluid helium coolant (hold the detectors at 1.8K and everything else at ~10K) was exhausted
 - first deep all-sky survey in the infrared
 - mapped the entire sky at wavelengths of 12, 25, 60, and 100um
 - point source catalog of over 245,000 sources
 - include a dust shell around Vega and 75,000 starburst galaxies
- follow-up missions were planned
- Infrared Space Observatory (ISO, 1995-1998)
 - Spitzer Space Telescope (2003-2020)
 - NICMOS (infrared instrument) placed on HST

11.2 INFRARED WAVEBANDS

11.2.1 Atmospheric windows

- H₂O and CO₂ absorb infrared radiation
 - H₂O absorption is sensitive to altitude
 - occurs in certain wavelength intervals (atmospheric windows)
 - **photometric bands**
- poor window X (30-35μm)
 - accessible from dry high-altitude sites or Antarctica
- some bands have variations
 - K_{short}: 2.0-2.3μm, K': 1.95-2.30μm, L': 3.5-4.1μm
- take care when compare photometric observations with those of other filters

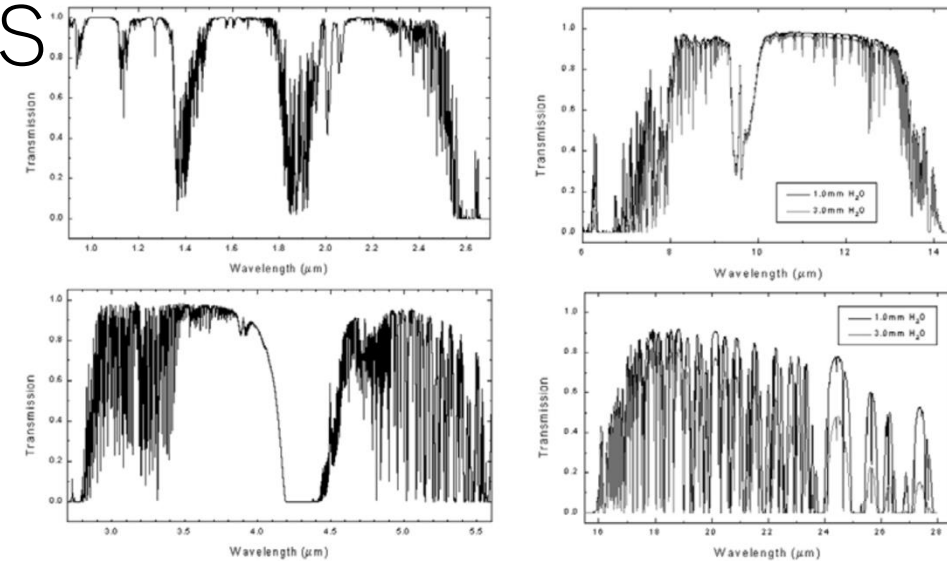


Figure 11.1. Details of the near-infrared transmission profile of the atmosphere above Mauna Kea (14,000 ft) for a typical water vapor level. Plots created using the ATRAN code developed by Steve Lord. Credit: Gemini Observatory web site.

Table 11.1. Infrared windows in the Earth's atmosphere.

Center wavelength (μm)	Designation of the bandwidth	Width (FWHM) (μm)
1.25	J	0.3
1.65	H	0.35
2.2	K	0.4
3.5	L	1.0
4.8	M	0.6
10.6	N	5.0
21	Q	11.0

11.2.2 The high-background problem

- major sources of unwanted background photons
 - **OH emission lines**
 - **black-body thermal emission** from the telescope
 - absolute temperature $T(K)$ → spectrum of the radiation from the Planck function $B_\lambda(T)$
 - emissivity $\varepsilon(\lambda)$ → fraction of black-body radiation added to the beam
 - Kirchhoff's Law $\varepsilon = 1 - R$ (R : measured spectral reflectivity)
- effective way to eliminate telescope background
 - **cool the entire telescope**
 - Mauna Kea(1°C), Antarctica($-13.6\sim-82.8^\circ\text{C}$), stratosphere(-50°C)

11.2.3 Chopping

- **chopping:** solution to the problem of a bright sky
 - “wobbling” (oscillating) secondary mirror in the telescope ($\sim 10\text{-}20\text{Hz}$)
 - rapidly switch between the source position on the sky and a reference position
 - typical wobbling secondary mirrors have a slow f/ratio
- in a photometer
 1. measure the total brightness of object+sky in the aperture
 2. record the signal from sky containing no objects in view by chopping
 3. eliminate sky signal from object+sky
 4. move the entire telescope every minute to measure the sky on the other side of the object (**nodding**)

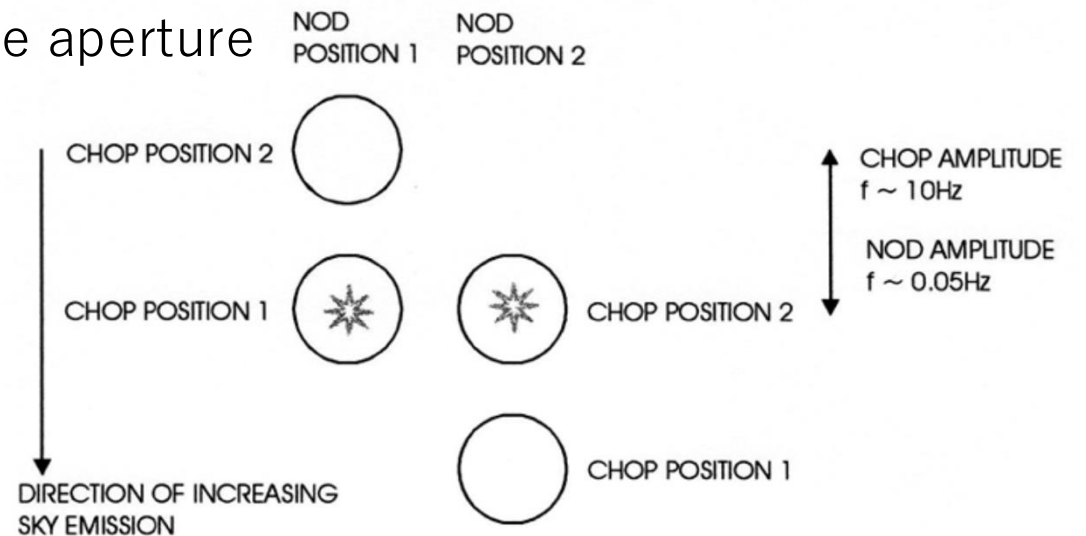


Figure 11.2. Chopping and nodding remove background flux and gradients at infrared wavelengths.

11.2.3 Chopping

- difference between the pair of chopped signals for nod position 1

$$\rightarrow C_1(x) = S + B_{tel,1} - B_{tel,2} + \left(\frac{d}{dx} B_{sky}\right) \Delta x$$

B_{tel} : telescope background at each chop position

B_{sky} : sky background at the chop positions

Δx : difference between chop position 1 and 2

- difference signal for nod position 2

$$\rightarrow C_2(x) = S - B_{tel,1} + B_{tel,2} - \left(\frac{d}{dx} B_{sky}\right) \Delta x$$

$$\rightarrow \text{required source signal } S = \frac{1}{2} (C_1(x) + C_2(x))$$

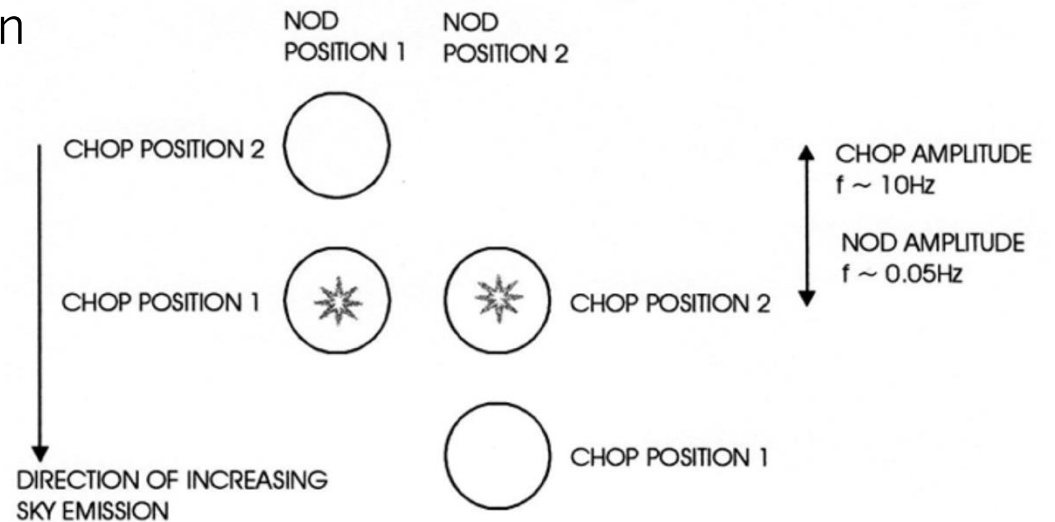


Figure 11.2. Chopping and nodding remove background flux and gradients at infrared wavelengths.

- $>3.5\mu\text{m}$: chopping and nodding are required for good background subtraction
- $<3.5\mu\text{m}$: only nodding is required

11.2.3 Chopping

- secondary mirror in infrared-optimized telescope
 - **slow f/ratio**
 - reduce the background on a detector pixel by stretching plate scale
 - **undersized** to permit chopping
 - the size of the secondary defines the entrance pupil of the system
 - **not surrounded by a black baffle**
 - subsequent image of the secondary is surrounded by sky which produces a lower background than black baffle
 - **gold-coated** : more reflective than aluminum in the IR
 - small **deflecting mirror** or **a hole** at the center of the secondary
 - eliminate thermal photons from the central Cassegrain

11.3 INFRARED ARRAY DETECTORS

11.3.1 The infrared “array” revolution, deja vu

- 1974-1984: construction of many forms of infrared array devices due to military applications
 - Koch et al (1981): InSb monolithic arrays
 - Kosonocky et al (1981): 256-element PtSi Schottky Barrier IR CCD line sensor
 - Baker et al (1981): 32×32 HgCdTe photovoltaic array hybridized to silicon circuitry
 - Rode et al (1981): hybrid arrays fabricated in HgCdTe or InAsSb and multiplexed to a Si CCD
 - Arens et al (1981, 1983): 32×32 pixels bismuth-doped silicon CID array at 10um
→astronomical observation (Arens et al 1984)
 - Dereniak et al (1984): 32×64 platinum silicide (PtSi) Schottky Barrier array
 - Niblack et al (1985): 32-element linear array of indium antimonide (InSb)
- ↔ • poor quantum efficiency
- high readout noise ($\sim 1,000$ electrons)
- small number of pixels

11.3.1 The infrared “array” revolution, deja vu

- other developments
 - Pipher and Forrest (1983): test of a 32×32 array of InSb detectors
 - astronomical results (Forrest et al 1985)
 - McLean and SBRC (1982-1984): 58×62 InSb array
 - noisier than desired to image using sub-arcsecond pixels, but still work
 - mid-1980s: development of MCT (HgCdTe or mercury-cadmium-telluride) for HST/NICMOS
 - can be customized to $\sim 2.5\mu\text{m}$
 - run at 77K and can be operated by CCD controllers
 - Petroff and Stapelbroek (1979): new way to construct extrinsic silicon photoconductors (BIB)
 - Spitzer and ground-based applications
 - 1986: **IRCAM** (58×62 InSb array) (UKIRT)
 - first light (1986/10)

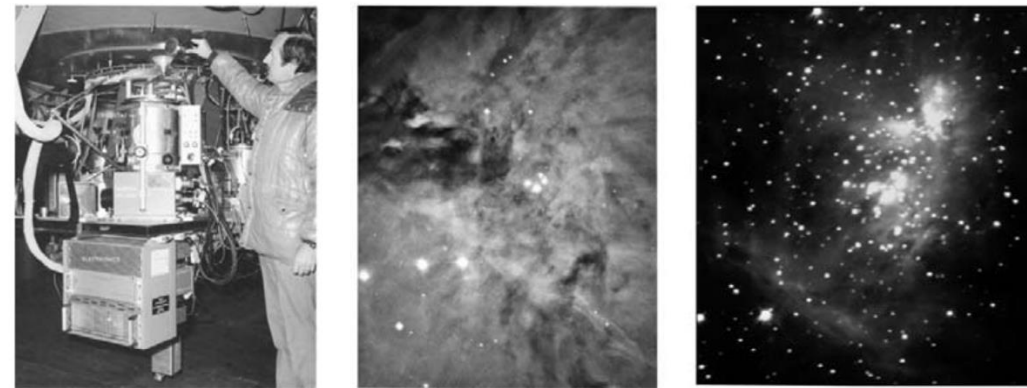


Figure 11.3. (Left) The author with IRCAM (1986), the first common-user camera system on the UKIRT 3.8 m infrared telescope to employ the 58×62 InSb arrays from SBRC (Raytheon). (Center) a visible light image of the Trapezium region of the Orion Nebula. (Right) An infrared image of the same region obtained with IRCAM at a wavelength of 2.2 microns. The bright source above the Trapezium is the Becklin–Neugebauer (BN) object. See also Plate 13.

11.3.1 The infrared “array” revolution, deja vu

- in 1993
 - NIR arrays : 256×256 , MIR arrays: 128×128 pixels
 - plans for $1,024 \times 1,024$ arrays were announced
- in 2008
 - NIR arrays : $2,048 \times 2,048$, MIR arrays: $1,024 \times 1,024$ pixels
 - Ge:Ga detectors for 70 and 160 μ m into 32×32 array for space applications
 - built into large mosaics for both cameras and spectrometers, or become the heart of complex instruments (diffraction-limited cameras and integral field spectrometers)

11.3.2 The hybrid structure

- to generate an infrared image
 1. convert radiation into electrical charge by the internal photoelectric effect or absorb the energy with a bolometer
 2. store the electrical charge at the site of generation (pixel)
 3. transfer the charge on each pixel to a single or a small number of outlets
 4. remove the charges as a voltage which can be digitized
 - each of the steps in infrared detection are so similar to those employed in a silicon CCD
 - ↔ difficult to manufacture infrared detector due to the limited experience in processing
- ⇒ **“hybrid” array**

11.3.2 The hybrid structure

- hybrid infrared array:
 - the functions of detecting infrared radiation and multiplexing the resulting electrical signal are separated → "sandwiches"
 - upper slab: **IR sensor** (InSb, HgCdTe, Si:As, Ge:Ga)
 - tightly packed grid of individual IR pixels (18-27 μ m)
 - lower slab: **silicon multiplexer**
 - electrically connected by tiny raised sections ("**bumps**") of an electrical conductor (indium)
 - indium: remain soft at low temperatures
 - gaps between the bumps are filled with an epoxy
 - to maintain the integrity of the sandwiches especially at low temperatures

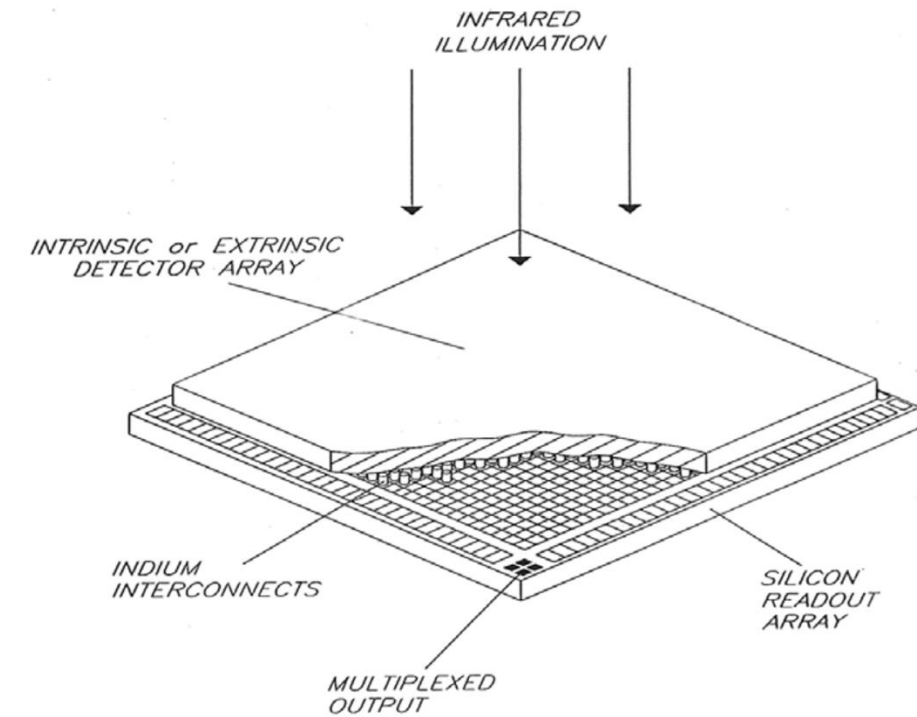


Figure 11.4. The "hybrid" structure of infrared array devices. The two slabs are separated by grid of tiny indium bumps that remain soft at cryogenic temperatures.

11.3.2 The hybrid structure

- access the signal from IR detector
 - microscopic array of “switches” made from MOSFETs
- charge storage
 - junction capacitance of the IR sensor (case of photodiode)
 - separate storage capacitor associated with the silicon circuitry
- entire structure: focal plane array (FPA), sensor chip assembly (SCA)
- silicon readout-integrated circuit chip: ROIC

- ways to multiplex the signal outputs from each unit cell
 - read each pixel sequentially by connecting signal to an output bus
 - use CMOS shift registers and more easily implemented
 - standard
 - access each pixel randomly for connection to the output amplifier
 - direct readout (DRO)
 - attractive but require more circuitry

11.3.2 The hybrid structure

- IR array are not based on charge-coupling principle
 - don't bleed along columns when a pixel saturates
 - bad pixels do not block off others in the same columns
 - "non-destructive" readout schemes are possible (effective)
 - on-chip charge binning and charge-shifting are not possible
- unit cell of an infrared array
 - **SFD** (source follower per detector)
 - contain a silicon field effect transistor (FET) as a source follower amplifier
 - provide a buffer for the accumulated charge in the pixel

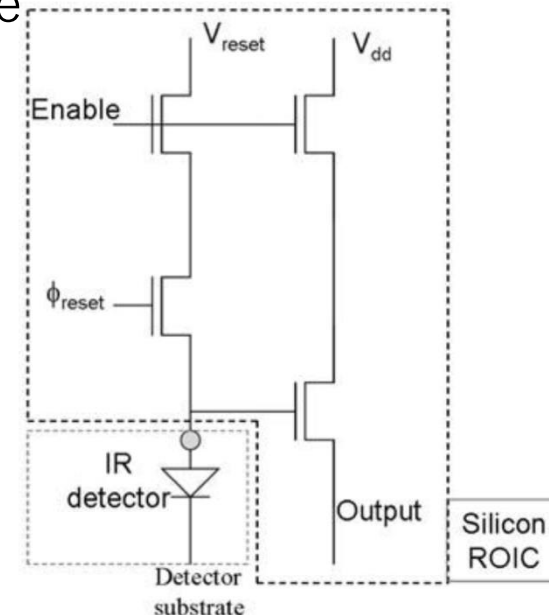


Figure 11.5. The “unit cell” of a typical near-infrared (photodiode) array; this is a four-transistor unit cell. Each detector has an output source follower and a reset switch, and there are two other FETs used for addressing the pixel.

11.3.2 The hybrid structure

- detection process

1. produce electron-hole pairs by the internal photoelectric effect

2. separate the electron-hole pair by an electric field

3. electrons move across the junction and the reverse bias decreases

→ discharge a capacitor

4. the amount of charge $Q = CV/e$

$e = 1.6 \times 10^{-19} C/e^-$: electrons, V : voltage across the detector, C : effective capacitance

5. each detector is connected to a source follower (SF) amplifier

$V_{out} = A_{SF}V_{in} \sim 0.7V_{in}$ (small loss of gain)

6. output voltage of SF can be read without affecting the input

7. reset the diode to the full reverse bias for next integration by another FET